

Peculiarities in Structural Behaviour of Graphite During Anionic Intercalation of PF_6^- , FSI^- and ClO_4^- at Elevated Temperature. Supplementary Information

Mikhail V. Gorbunov* and Daria Mikhailova

Leibniz Institute for Solid State and Materials Research (IFW Dresden), Helmholtzstraße 20, 01069, Dresden, Germany. m.gorbunov@ifw-dresden.de

Experimental

Operando experiments were conducted in custom-made coin cells with glass windows. To inhibit the corrosion of stainless-steel cathode current collectors at high voltages, they were covered by a 50 nm layer of titanium beforehand, using the magnetron. However, this procedure was insufficient and other anti-corrosive measures are required, e.g. the one described in the ref. 15 of the article. Not only the electrolyte stability at elevated temperature is an issue, but also the impact of the current collectors' corrosion grows.

Electrolytes were the following: 4m LiPF_6 (Sigma Aldrich, 99.9% purity) dissolved in DMC (Sigma Aldrich, >99% purity); 3m LiClO_4 (Sigma Aldrich, 99.99% purity) dissolved in the mixture of 47.5 mass% PC (Sigma Aldrich, 99.7% purity), 47.5 mass% DMC and 5 mass% FEC (Thermo Fischer Scientific, >98% purity); 7m LiFSI (TCI Chemicals, >98% purity) dissolved in DMC. In this study, we deliberately used electrolyte solvents of a similar chemical nature, which allowed to discuss the possibility of solvent co-intercalation. Selection of alternative electrolytes which would sustain high voltages in a broad temperature range is challenging. For example, solutions of 2m LiFSI and LiPF_6 in ethyl methyl sulfone (EMS) are possible to prepare, whereas solubility of LiClO_4 in EMS is low.

Electrode materials for the *operando* studies represented commercial graphite (KS6L, Imerys) mixed with PTFE (Sigma Aldrich) in the mass ratio of 9:1 using an agate mortar. The latter was pressed onto Al mesh using a hydraulic press. The applied pressure was around $3\text{ t}\cdot\text{cm}^{-2}$. Glass fibre (Whatman) soaked in a corresponding electrolyte served as a separator, and metallic lithium as a counter electrode. All the preparation was done in an Ar-filled glovebox (MBraun) with oxygen and water vapor concentration below 1 ppm. *Operando* X-ray diffraction study was performed at the beamline BL04-MSPD of ALBA synchrotron (Spain)^{33, main} using the specially dedicated sample holders for room^{34, main} and elevated^{35, main} temperatures. The holders were connected to VMP3 potentiostat (Biologic, France), and electrochemical cells were cycled at relatively high current densities to reduce the impact of parasitic reactions related to corrosion of the coin cell parts, especially at elevated temperatures. The use of High-throughput Position Sensitive Detector MYTHEN in combination with the mentioned sample environment allowed to collect one X-ray diffractogram within 10 minutes. Galvanostatic charge-discharge curves corresponding to *operando* diffractograms shown in the article text are presented in Figure S1.

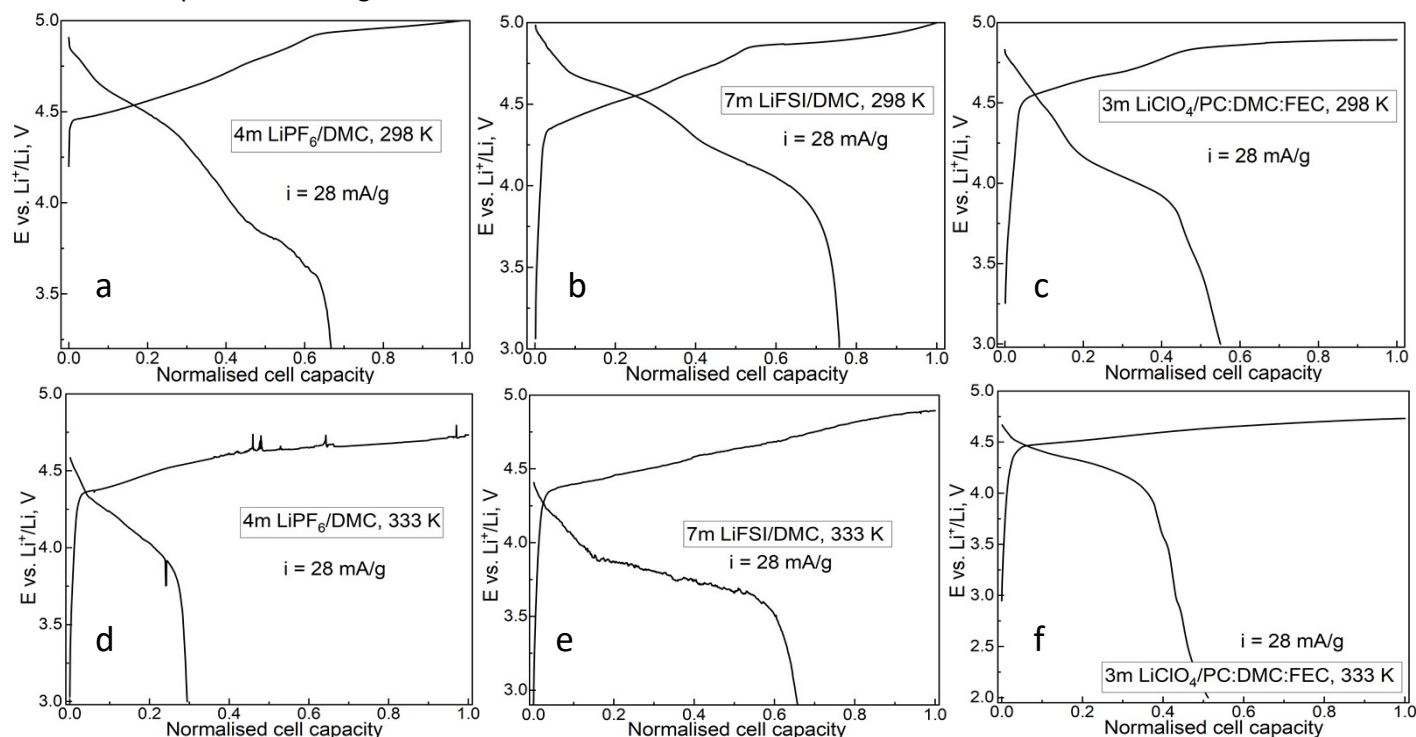


Figure S1. Galvanostatic charge-discharge curves corresponding to the *operando* XRD experiments. Note, that for 7m LiFSI /DMC (panel b), only the curve relating to full charge-discharge (stage 2) is shown, and for perchlorate system (panels c, f), the curves are shown only for the first charge-discharge cycles with a purpose of saving the space.

Comments on the Structural Analysis

Note that in the cited literature, error bars for the interlayer spacing were either not given or it was calculated from the data available in the literature (X-ray diffractograms). In our experimental results, the last significant digit was the fourth after the decimal separator. We rounded all the obtained values to the third digit for proper comparison.

Figure S2 is showing a simplified general model for the MIC stage for intercalation of FSI^- anions with $n = 1.75$. As specified in the main text, one can see alternating of galleries with or without intercalant in between the graphene layers. Co-existence of multiple intercalation stages would result in a non-integer number obtained using the equation 1. If every space between the graphene layers is occupied, the n is equal to 1, and the reflection $00n+1$ on the X-ray diffractogram should disappear. This was observed for PF_6^- anions, however, the nature of the process remains discussable and the detailed investigation on this is planned for the future. We introduced the MIC term for the both cases. Another reason for the observed phenomena might be a mixture of two mechanisms specified in the main article text: sequential and random statistical filling of the interlayer spaces. With temperature increase, random distribution of the guest species could be expected, since contribution of the entropy factor to the Gibbs free energy of the system should increase accordingly. Also, an attention has to be paid to the fact that changes in the intercalation mechanism induced by temperature might be different for various graphitic materials, depending on their initial interlayer spacing, which would represent an interesting and broad direction to explore.

Anionic diffusion

To evaluate the changes in apparent diffusion coefficient of PF_6^- in bulk graphite during intercalation presented in Figure 3 of the main article, we performed galvanostatic intermittent titration experiment (GITT) in a 3-electrode Swagelok-type cell. Metallic lithium served as counter and reference electrodes. The electrolyte was 2m LiPF_6 dissolved in ethyl methyl sulfone (TCI chemicals, 98% purity). Current pulse corresponding to a current density of $40 \text{ mA} \cdot \text{g}^{-1}$ was applied for 600 seconds, followed by relaxation time of 2 hours. The values of diffusion coefficients were calculated using the Weppner-Huggins¹ formula:

$$D = \frac{4}{\pi} \left(\frac{m \cdot V_m}{M \cdot A} \right)^2 \cdot \left(\frac{\Delta E_s}{\tau \cdot \left(\frac{dE}{d\sqrt{t}} \right)} \right)^2$$

Here, M and m are the molar mass and mass of active material (graphite). A is the area of electrode, however, it represents a geometrical value instead of the real active area, which is larger, and thus the diffusion coefficients are slightly overestimated. V_m stands for the molar volume of graphite. ΔE_s represents the difference of the open circuit potentials before and after the current pulse. Each three subsequently obtained values were averaged to ensure the reliability. Note, this experiment was conducted only at room temperature.

Figure S3 is referring to the same *operando* experiment for PF_6^- intercalation, but using a sulfone-based electrolyte. Since it was conducted within the framework of a project dedicated to potassium-ion batteries, a potassium salt KPF_6 was used. However, the process of anionic intercalation remained unchanged, therefore, we consider it relevant for comparison. Unfortunately, the selected electrolyte concentration was not optimal, thus the reflections which correspond to staging are hindered by those of crystallo-solvates (which dissolved slowly during the experiment at 333 K) as well as Al grid/metallic potassium. Nevertheless, they are still distinguishable and pointed correspondingly.

In parallel to the *operando* XRD studies, an attempt of evaluating the kinetics of anionic (de)intercalation for PF_6^- was done. Note that evaluation of the temperature to 333 K was not performed in the series of the preliminary electrochemical studies because of corrosion issues influencing the values of the obtained diffusion coefficients.

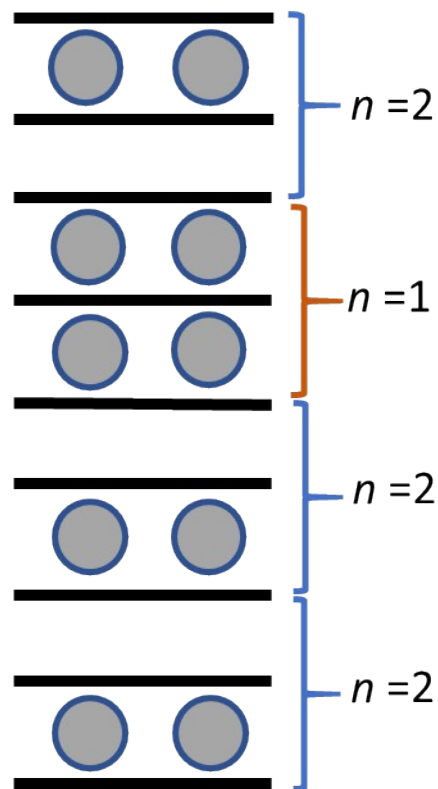


Figure S2. A simplified model for intercalation stage with a non-integer number.

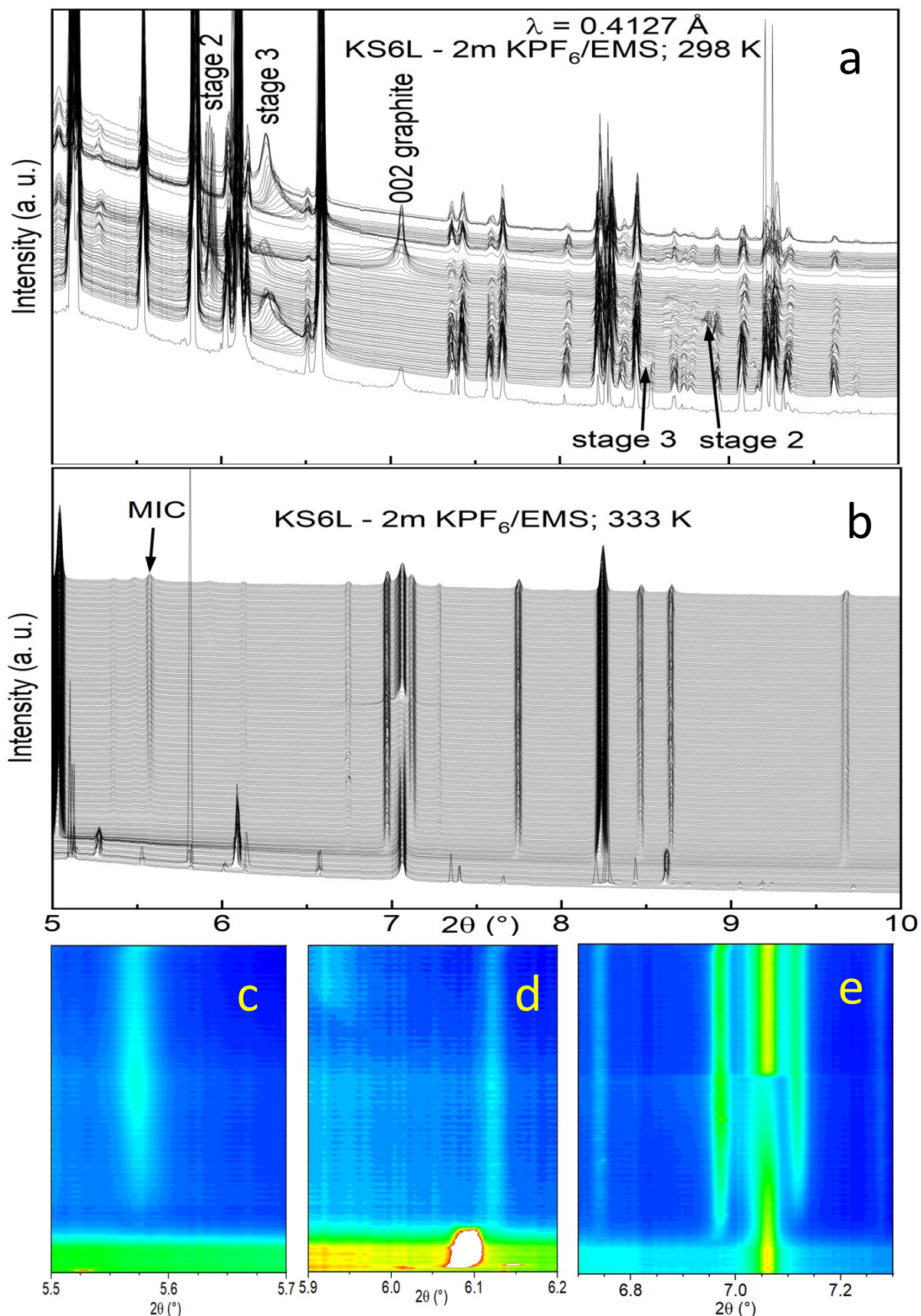


Figure S3. Operando XRD studies of PF_6^- intercalation into graphite from sulfone-based potassium electrolyte at (a) room and (b) elevated temperature. Panels (c-e) represent colour maps for panel (b), highlighting the reflections of graphite intercalation stages which were strongly hindered, as already described. Panel (c) corresponds to MIC stage, panel (d) to stage number approaching the value of 3, and panel (e) stands for (002) reflection of graphite and reflections of an intercalation stage with a high n value.

For estimating the activation barrier for PF_6^- anions diffusion in bulk graphite, differential capacity plots were built to obtain the approximate values for diffusion coefficients. The results of the GITT experiment at 298 K showed in the main article additionally served as the validity criterium. Randles-Sevcik equation was applied².

$$i_{\square} = 0.4463 \left(\frac{F^3}{RT} \right)^{1/2} n^{3/2} s D_O^{1/2} c_O v^{1/2}$$

We considered the best-resolved peaks from charge and discharge parts of the curves (around 5.25 V) shown in panels c-e of the Figure S4 for building the Arrhenius plot (panel f). Estimations of the diffusion coefficients for cell charge at 298 K obtained by the Randles-Sevcik and Weppner-Huggins formulas are in good agreement: $5.1 \cdot 10^{-11} \text{ cm}^2/\text{s}$ vs. $5.4 \cdot 10^{-11} \text{ cm}^2/\text{s}$, concerning the systematic error. In both methods, the geometrical electrode area was used instead of the real parameter, which would account for the specific surface of the material. The values of E_A obtained for charge and discharge almost coincide with those from the theoretical calculations^{27, main}: 0.15(3) vs. 0.150 eV. Also, the corrosion impact on the results is present (see the irreversible specific capacity in panel b). In the end, these results serve as the starting point, and the measurements will be completed using a specifically dedicated equipment.

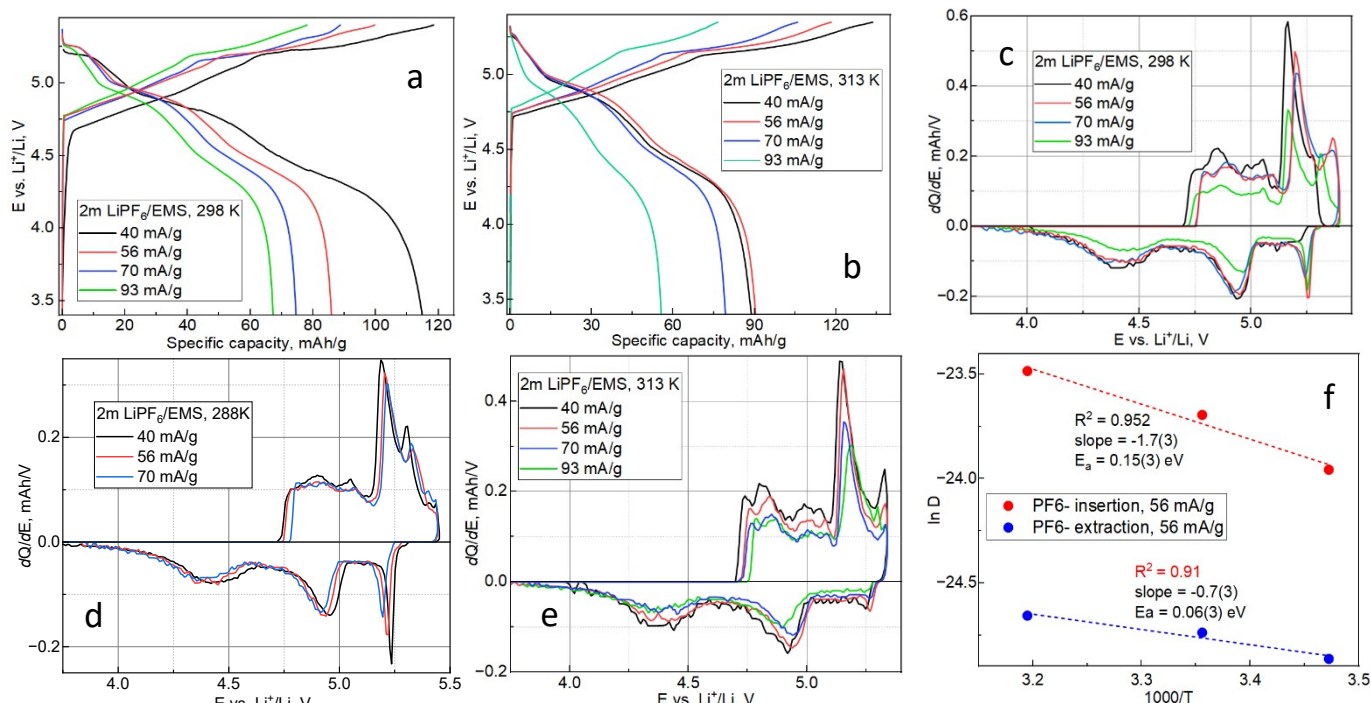


Figure S4. Estimation of the barriers for PF_6^- anions' diffusion in bulk graphite by the Randles-Sevcik method, considering it as the limiting stage. (a, b) – galvanostatic charge-discharge curves obtained in EMS-based electrolytes at different temperatures, illustrating the impact of corrosion; (c–e) – differential capacity plots for three temperatures, (f) – Arrhenius plots obtained from the D values and E_A estimations. Insufficient correlation coefficient R^2 in panel f is highlighted by red colour.

1. W. Weppner, R. A. Huggins, *J. Electrochem. Soc.* **1977**, *124*, 1569–1578.
2. A. J. Bard, L. R. Faulkner, “Electrochemical Methods: Fundamentals and Applications”, 2nd ed., Wiley, **2001**.

Acknowledgements

We acknowledge Dina Biberstein (IFW Dresden) for the magnetron sputtering of *operando* coin cells. This research has benefitted from beamtime allocation at BL04-MSPD at ALBA Synchrotron (Spain)³ and the specific equipment for *operando* XRD in a battery setup^{4–5}. Financial support was done by DFG project 448719339 (KIBSS).

3. F. Fauth, I. Peral, C. Popescu, et al., *Powd Diff.*, **2013**, *28*, 360.
4. M. Herklotz, J. Weiß, E. Ahrens et al., *J. Appl. Crystallogr.*, **2016**, *49*, 340.
5. R. G. Houdeville, A. Missyul, V. Fuentes, et. al, *J. Electrochem. Soc.*, **2024**, *171*, 010533.